Adaptive Feedback Linearization Controller for Stabilization of Quadrotor UAV

Ahmed Eltayeb[1], Mohd Fuaad Rahmat[1]*, Mohd Ariffanan Mohd Basri[1]

[1]School of Electrical Engineering, faculty of Engineering,
Universiti Teknologi Malaysia, 81310 Skudai, Johor, MALAYSIA

*Corresponding Author

Abstract: Due to the various applications of the quadrotor unmanned aerial vehicle (UAV) systems increase daily, the researchers recently granted it considerable attention. In this manuscript, the mathematical model of the quadrotor UAV has been presented. The feedback linearization (FBL) technique is implemented to linearize the attitude and altitude dynamic equations of the quadrotor UAV. The proportional-integral-derivative (PID) controller is designed to the obtained linearized model (attitude and altitude subsystems). The quadrotor UAV that used for outdoor applications is influenced by the wind guest disturbances and parameter uncertainties, which result in the deterioration of the PID controller performance, and gain re-tuning is required. Therefore, for a robust performance against the wind disturbance and the parameter uncertainties, the adaptive feedback linearization (AFBL) is proposed and implemented to stabilize the quadrotor attitude and altitude subsystems. The parameter uncertainties have been adaptively estimated based on the Lyapunov stability function, which was able to cancel the quadrotor system uncertainties. The proposed controller has been evaluated by simulation Matlab/Simulink and provided better performance against parameter uncertainties and wind guest disturbances, where the error in the attitude and altitude have been reduced about % 82 and % 53, respectively, compared to the conventional exact FBL controller.

Keywords: Quadrotor UAV, adaptive feedback linearization, PID control, lyapunov function.

1. Introduction

Unmanned Aerial Vehicle quadrotor (UAV) is an aircraft operated without a human pilot on board. Earlier, the UAVs came-up with the large size, which results in the expensive cost for the design. However, the recent technologies in such as batteries, electronics, mechatronics, etc. result in small and cheap UAVs that can be used for civilian and military applications effectively. The Newton-Euler formalism is commonly used to drive the mathematical model of the quadrotor [1]–[4]. Then, depends on the control design requirements, the driven model is put in various mathematical expressing to describe the translational and the rotational dynamics of the quadrotor UAV.

The description of various representations of the quadrotor dynamics is presented, and from the trajectory tracking point of view, the problem of computing desired roll and pitch angles is discussed, which are basically the virtual signals derived to achieve the desired position. In addition, the review of the quadrotor control design (linear and non-linear controllers) such as in are presented to provide a better understanding of the quadrotor control design and experiments. Various types of flight test-beds were shown to validate the controller [5].

The quadrotor is an under-actuated, nonlinear, and unstable system; these complex characteristics lead to a challenge in the control design stage. Therefore, many control techniques are implemented for the quadrotor in the literature, such as the proportional-integral-derivative (PID) controller, which widely used to control the quadrotor systems because of its simplicity in the implementation [6]–[9]. Ataka et al [10] developed a linear model of the quadrotor at some equilibrium points, then the controllability and observability testing of the extracted linear model was done as well. Madani et al [11] divided the quadrotor system into three subsystems and then applied the backstepping control to stabilize the whole system.

Mukherjee et al [12] derived a direct adaptive feedback linearization for quadrotor and the stability tested by using the Lyapunov theory. Lee et al. [13] applied two nonlinear control methods on quadrotor UAV, a feedback linearization, and adaptive sliding mode controllers. Voos [14] designed the controller based on decomposition into a nested structure, and then the feedback linearization is implemented to the quadrotor system. The attitude controller is designed based on quantitative feedback theory, and then, a fuzzy logic controller is applied to provide position trajectory tracking for the quadrotor [15], [16].

In this paper, the dynamic model of quadrotor UAV has been mathematically presented. The exact feedback linearization technique is used to linearize the attitude dynamic equations of the quadrotor. The PID controller has been implemented to the obtained linear model (attitude and altitude subsystems). However, due to the nature of the quadrotor applications (outdoor applications) in which the quadrotor will be subjected to the wind guest disturbance and parameter uncertainties, therefore, a robust controller is required to overcome these challenges. The adaptive feedback linearization is proposed and implemented to the quadrotor attitude and altitude subsystems for a robust performance against the wind disturbance rejection and the model parameter uncertainty. The stability approach of the proposed controller has been derived based on the elected Lyapunov theory. The proposed controller (adaptive feedback linearization) has been envaulted by simulation using MATLAB/SIMULINK platform in the presence of wind guest disturbance rejection and parameter uncertainty. The performance of the proposed controller has been compared with the conventional exact feedback linearization in terms of the trajectory tracking error, and the presented simulation results showed significant improvement.

The paper is organized as follows, started with section one, the introduction. Section two is dedicated to the quadrotor modeling. While section three introduced the feedback linearization technique. In section four, the proposed adaptive feedback linearization controller is designed for the quadrotor system to enhance the control system performance against the wind gust disturbance rejection and the model parameter uncertainty. Section five presented the detailed simulation results by using Matlab/Simulink platform. Finally, section six concluded the paper.

2. Illustrations

2.1 Quadrotor Description

The quadrotor UAV consists of four rotors to generate the propeller forces (F_1, F_2, F_3, F_4), these rotors are mounted in a cross configuration and in symmetric shape, as shown in Fig. 1.
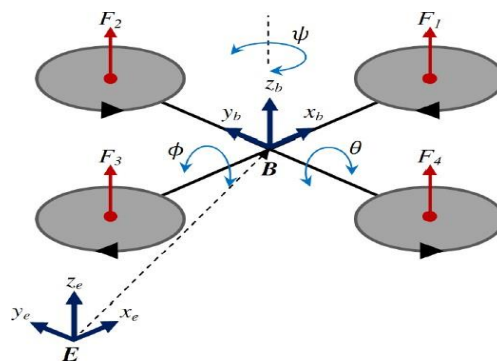

Fig. 1 - Quadrotor UAV configuration

Basically, the quadrotor movements are controlled by changing the speed of the rotors (called control inputs), and the idea is based on dividing these four rotors into two groups/pairs, the front and the rear rotors (1, 3), and the left and the right rotors (2, 4), respectively as depicted in Fig. 2. By convention, Rotors (1, 3) rotate in a clockwise direction, while rotors (2, 4) rotate in the anti-clockwise direction.
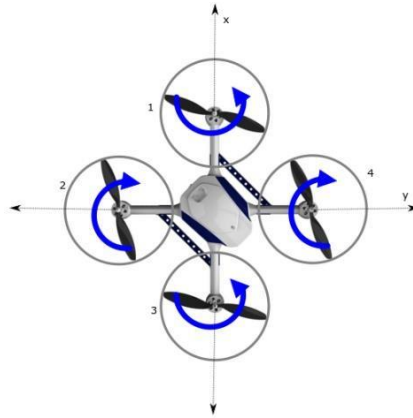
Fig. 2 - Rotors numbering in an anticlockwise direction

The quadrotor moves in a vertical direction by increasing or decreasing the angular velocities of all 4 rotors with the same speed simultaneously, which results in producing a total lift force (thrust) against the gravity force. Therefore, the quadrotor will take-off, as shown in Fig. 3 (a) or landing, as depicted in Fig. 3 (b).
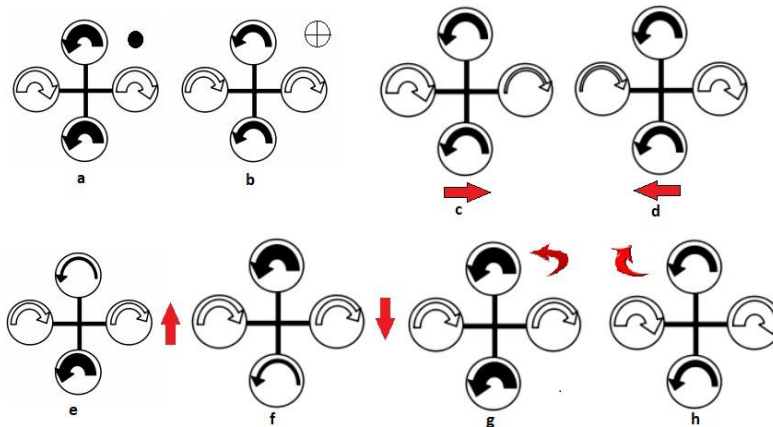

Fig. 3 - Quadrotor UAV possible motions

The right direction movement of the quadrotor is achieved by increasing the rotational speed of the rotor (2) and decreasing the rotational speed of the rotor (4), as the result of that the quadrotor will move in the right direction as shown in Fig. 3 (c). Similarly, the left direction movement of the quadrotor is achieved by increasing the rotational speed of the rotor (4) and decreasing the rotational speed of the rotor (2); as a result, the quadrotor will move in the left direction as shown in Fig. 3 (d). The right and left movements of the quadrotor are controlled by changing the roll angle (ϕ) of the quadrotor.

The forward movement of the quadrotor is achieved by increasing the rotational speed of the rotor (3) and decreasing the rotational speed of the rotor (1); as a result, the quadrotor will move in the forward direction as illustrated in Fig. 3 (e). Similarly, the backward movement of the quadrotor is achieved by increasing the rotational speed of the rotor (1) and decreasing the rotational speed of the rotor (3); as a result, the quadrotor will move in the backward direction as shown in Fig. 3 (f). The forward and backward movements of the quadrotor are controlled by changing the pitch angle (θ). Finally, the anti-clockwise and clockwise movements of the quadrotor are controlled by changing yaw angle (ψ) as shown in Fig. 3 (g & h), respectively.

2.2   Quadrotor UAV Kinematic Model

Generally, there are two frames: earth fixed frame (E-frame) denoted by $E = (x_e, y_e, z_e)$ and body fixed (B-frame) $B = (x_b, y_b, z_b)$, as depicted in Fig. 1.

Assume that $q = (x, y, z, \phi, \theta, \psi) \in R^6$ represents generalized coordinates of the quadrotor, where (x, y, z) represents the quadrotor position while (ϕ, θ, ψ) are the three Euler angles (literally are roll, pitch, and yaw) which describe the quadrotor orientation. Thus, the quadrotor mathematical model can be represented into two coordinate subsystems: the translational and the rotational subsystems. Therefore, the generalized coordinates of the quadrotor can be re-written as follows:

$$q = [\xi, \eta]^T \tag{1}$$

where,

$$\xi = [x, y, z]^T \tag{2}$$

and,

$$\eta = [\phi, \theta, \psi]^T \tag{3}$$

Therefore, the kinematic equations can be obtained as follows:

$$\dot{\xi} = RV \tag{4}$$

Where, $\dot{\xi}$ and V represent the linear velocity vectors in both frames the E-frame and B-frame, respectively. And R is the rotation matrix:

$$R = \begin{bmatrix} \cos\theta\cos\psi & \sin\phi\sin\theta\cos\psi - \cos\phi\cos\psi & \sin\phi\sin\theta\cos\psi + \cos\phi\sin\psi \\ \cos\theta\sin\psi & \sin\phi\sin\theta\sin\psi + \cos\phi\cos\psi & \cos\phi\sin\theta\sin\psi - \sin\phi\cos\psi \\ -\sin\theta & \sin\phi\cos\theta & \cos\phi\cos\theta \end{bmatrix} \tag{5}$$

The quadrotor rotational movements are obtained as follows:

$$\dot{\eta} = T\omega \tag{6}$$

where, $\dot{\eta}$ and ω represent the angular velocity vector with respect to the E-frame and B-frame, respectively. T is the transfer matrix [17]:

$$T = \begin{bmatrix} 1 & \sin\phi\tan\theta & \cos\phi\tan\theta \\ 0 & \cos\phi & -\sin\phi \\ 0 & \dfrac{\sin\phi}{\cos\theta} & \dfrac{\cos\phi}{\cos\theta} \end{bmatrix} \tag{7}$$

2.3 Quadrotor Dynamic Model

The Newton-Euler method has been used in this section to drive the quadrotor's translational and rotational dynamic equations. The translational dynamic equation will be expressed with respect to E-fame, while the rotational dynamic equation will be expressed with respect to B-frame.
The translational dynamic equations can be expressed as follows:

$$m\ddot{\eta} = mge_z + u_T Re_z \tag{8}$$

where m represents the mass of the quadrotor, g is the gravity acceleration, $e_z = [0,0,1]^T$ is the unite vector along the z- axis and u_T is the total lift force produced by the four rotors and it's defined as follows:

$$u_T = \sum_{i=1}^{4} F_i = b \sum_{i=1}^{4} \Omega_i^2 \tag{9}$$

Where F_i and Ω_i represent the thrust force and the speed of rotor i, respectively, b is the thrust factor. The rotational dynamic equations can be expressed as follows:

$$I\dot{\omega} = -\omega \times I\omega - G_a + \tau \tag{10}$$

where I represent the inertia matrix, $(\omega \times I\omega)$ and G_a are the gyroscopic effect, while τ is the control inputs. G_a and τ are defined as:

$$G_a = \sum_{i=1}^{4} J_r \, (\omega \times e_z)(-1)^{i+1} \omega_i \qquad (11)$$

and,

$$\tau_a = \begin{bmatrix} \tau_\phi \\ \tau_\theta \\ \tau_\psi \end{bmatrix} = \begin{bmatrix} lb(\Omega_4^2 - \Omega_2^2) \\ lb(\Omega_3^2 - \Omega_1^2) \\ d(\Omega_4^2 + \Omega_2^2 - \Omega_3^2 - \Omega_1^2) \end{bmatrix} \qquad (12)$$

Where J_r is the rotor inertia, l is the distance between the center of the quadrotor and the center of a rotor, and b is the drag factor.

Thus, from (8) and (10) the overall dynamic equations in terms of position ξ and rotation of the quadrotor body can be put as follows:

$$\begin{bmatrix} \ddot{x} \\ \ddot{y} \\ \ddot{z} \end{bmatrix} = \begin{bmatrix} 0 \\ 0 \\ -g \end{bmatrix} + \frac{1}{m} \begin{bmatrix} \cos\phi \sin\theta \cos\psi + \sin\phi \sin\psi \\ \cos\phi \sin\theta \cos\psi - \sin\phi \sin\psi \\ \cos\phi \cos\theta \end{bmatrix} \qquad (13)$$

$$\begin{bmatrix} \ddot{\phi} \\ \ddot{\theta} \\ \ddot{\psi} \end{bmatrix} = \begin{bmatrix} \dot{\theta}\dot{\psi}\dfrac{I_y - I_z}{I_x} \\ \dot{\phi}\dot{\psi}\dfrac{I_z - I_x}{I_y} \\ \dot{\theta}\dot{\psi}\dfrac{I_x - I_y}{I_z} \end{bmatrix} - \begin{bmatrix} \dot{\theta}\Omega_d\dfrac{J_r}{I_x} \\ -\dot{\phi}\Omega_d\dfrac{J_r}{I_y} \\ 0 \end{bmatrix} + \begin{bmatrix} \dfrac{1}{I_x}\tau_\phi \\ \dfrac{1}{I_y}\tau_\theta \\ \dfrac{1}{I_z}\tau_\psi \end{bmatrix} \qquad (14)$$

Finally, the overall dynamic equations of quadrotor UAV in 6-DOF can be written as follows:

$$\begin{aligned} \ddot{x} &= \frac{\cos\phi \sin\theta \cos\psi + \sin\phi \sin\psi}{m} u_4 \\ \ddot{y} &= \frac{\cos\phi \sin\theta \cos\psi - \sin\phi \sin\psi}{m} u_4 \\ \ddot{z} &= -g + \frac{\cos\phi \cos\theta}{m} u_4 \\ \ddot{\phi} &= \dot{\theta}\dot{\psi}\frac{I_y - I_z}{I_x} + \dot{\theta}\Omega_d\frac{J_r}{I_x} + \frac{1}{I_x} u_1 \\ \ddot{\theta} &= \dot{\phi}\dot{\psi}\frac{I_z - I_x}{I_y} + \dot{\phi}\Omega_d\frac{J_r}{I_y} + \frac{1}{I_y} u_2 \\ \ddot{\psi} &= \dot{\theta}\dot{\psi}\frac{I_x - I_y}{I_z} + \frac{1}{I_z} u_3 \end{aligned} \qquad (15)$$

Where u_1, u_2, u_3, u_4 are the control inputs of the quadrotor UAV system and have the following formula:

$$\begin{aligned} u_1 &= b(\Omega_4^2 - \Omega_2^2) \\ u_2 &= b(\Omega_3^2 - \Omega_1^2) \\ u_3 &= d(\Omega_4^2 + \Omega_2^2 - \Omega_3^2 - \Omega_1^2) \\ u_4 &= b(\Omega_1^2 + \Omega_2^2 + \Omega_3^2 + \Omega_4^2) \end{aligned} \qquad (16)$$

5

While Ω_d represents the disturbance, and expressed as follows:

$$\Omega_d = -\Omega_1 + \Omega_2 - \Omega_3 + \Omega_4 \tag{17}$$

The control inputs (16) can be written in a matrix as:

$$\begin{bmatrix} u_1 \\ u_2 \\ u_3 \\ u_4 \end{bmatrix} = \begin{bmatrix} b & b & b & b \\ 0 & -b & 0 & b \\ -b & 0 & b & 0 \\ -d & d & -d & d \end{bmatrix} \begin{bmatrix} \Omega_1^2 \\ \Omega_2^2 \\ \Omega_3^2 \\ \Omega_4^2 \end{bmatrix} \tag{18}$$

$$\begin{bmatrix} \Omega_1^2 \\ \Omega_2^2 \\ \Omega_3^2 \\ \Omega_4^2 \end{bmatrix} \begin{bmatrix} 0.25 & 0 & -0.5 & -0.25 \\ 0.25 & -0.5 & 0 & 0.25 \\ 0.25 & 0 & 0.5 & -0.25 \\ 0.25 & 0.5 & 0 & 0.25 \end{bmatrix} \begin{bmatrix} \dfrac{u_1}{b} \\ \dfrac{u_2}{b} \\ \dfrac{u_3}{b} \\ \dfrac{u_4}{b} \end{bmatrix} \tag{19}$$

3. Feedback Linearization

The feedback linearization method for attitude and altitude control of the quadrotor UAV system is presented in this section. Simply, the feedback linearization method uses to transfer the nonlinear systems to an equivalent linear system, which can be handled easily. The quadrotor non-linear dynamic equations (20) can be written in a generic non-linear systems formula as in (21), which can be converted to a linear system by applying equation (22). Therefore, the quadrotor attitude and altitude linear system are obtained as in (25), and the overall linearized model is depicted in Fig. **4**.
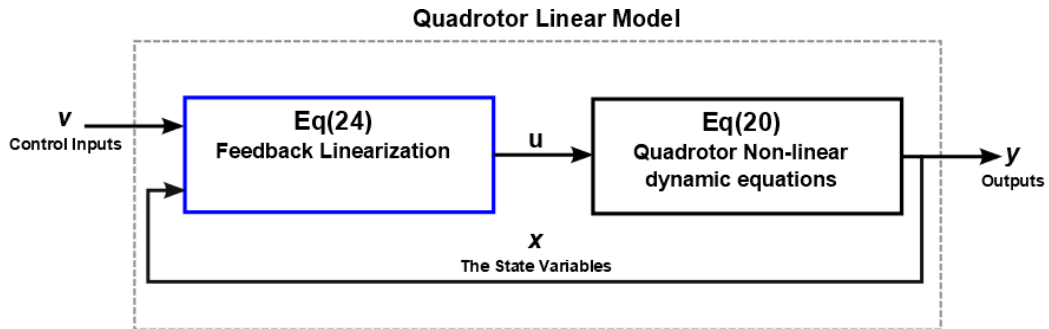

Fig. 4 - Linearized model

The attitude and altitude quadrotor UAV subsystem dynamic equations are:

$$\ddot{\phi} = \dot{\theta}\dot{\psi}\frac{I_y - I_z}{I_x} + \dot{\theta}\Omega_d\frac{J_r}{I_x} + \frac{1}{I_x}u_1$$

$$\ddot{\theta} = \dot{\phi}\dot{\psi}\frac{I_z - I_x}{I_y} + \dot{\phi}\Omega_d\frac{J_r}{I_y} + \frac{1}{I_y}u_2$$

$$\ddot{\psi} = \dot{\theta}\dot{\psi}\frac{I_x - I_y}{I_z} + \frac{1}{I_z}u_3$$

$$\ddot{z} = -g + \frac{\cos\phi\cos\theta}{m}u_4$$

$$\tag{20}$$

The feedback linearization for a class of non-linear system as in (21), can be done as follows:

$$\dot{x} = f(x) + Gu \tag{21}$$

Where x is the state vector, $f(x)$ is the non-linear function (vector), and the control input u which can be selected in such a way to cancel all non-linear terms in (21) and leads to the linear system. Therefore, u can be chosen as follows:

$$u = G^{-1}(-f(x) + v) \tag{22}$$

By substituting (22) into (21) leads to a linear system:

$$\dot{x} = v \tag{23}$$

Thus, by following the same procedures, the control inputs u_1, u_2, u_3 and u_4 in (20) can be selected as follows:

$$
\begin{aligned}
u_1 &= \frac{1}{b_1}(-a_1 \dot{\theta}\dot{\psi} - a_2 \dot{\theta}\Omega_d + v_1) \\
u_2 &= \frac{1}{b_2}(-a_3 \dot{\phi}\dot{\psi} - a_4 \dot{\phi}\Omega_d + v_2) \\
u_3 &= \frac{1}{b_3}(-a_5 \dot{\theta}\dot{\phi} + v_3) \\
u_4 &= \frac{m}{\cos \phi \cos \theta}(g + v_4)
\end{aligned}
\tag{24}
$$

where,

$$a_1 = \frac{I_y - I_z}{I_x}, a_2 = \frac{J_r}{I_x}, a_3 = \frac{I_z - I_x}{I_y}, a_4 = \frac{J_r}{I_y}, a_5 = \frac{I_x - I_y}{I_z}$$

$$b_1 = \frac{l}{I_x}, b_2 = \frac{l}{I_y}, b_3 = \frac{1}{I_z}$$

Therefore, by substituting (24) into (20) leads to the following linear systems:

$$
\begin{aligned}
\ddot{\phi} &= v_1 \\
\ddot{\theta} &= v_2 \\
\ddot{\psi} &= v_3 \\
\ddot{z} &= v_4
\end{aligned}
\tag{25}
$$

The nonlinear dynamic attitude and altitude model is transformed into an equivalent linear, and the state space of representation of the linearized model can be written as follows:

$$\dot{x} = Ax + Bu \tag{26}$$

The output is:

$$y = Cx \tag{27}$$

where the state variables are:

$$x = [\varphi \quad \dot{\varphi} \quad \theta \quad \dot{\theta} \quad \psi \quad \dot{\psi} \quad z \quad \dot{z}]$$

and,

$$
A = \begin{bmatrix} 0 & 1 & 0 & 0 & 0 & 0 & 0 & 0 \\ 0 & 0 & 0 & 0 & 0 & 0 & 0 & 0 \\ 0 & 0 & 0 & 1 & 0 & 0 & 0 & 0 \\ 0 & 0 & 0 & 0 & 0 & 0 & 0 & 0 \\ 0 & 0 & 0 & 0 & 0 & 0 & 1 & 0 \\ 0 & 0 & 0 & 0 & 0 & 0 & 0 & 0 \\ 0 & 0 & 0 & 0 & 0 & 0 & 0 & 1 \\ 0 & 0 & 0 & 0 & 0 & 0 & 0 & 0 \end{bmatrix}, B = \begin{bmatrix} 0 & 0 & 0 & 0 \\ 1 & 0 & 0 & 0 \\ 0 & 0 & 0 & 0 \\ 0 & 1 & 0 & 0 \\ 0 & 0 & 0 & 0 \\ 0 & 0 & 1 & 0 \\ 0 & 0 & 0 & 0 \\ 0 & 0 & 0 & 1 \end{bmatrix}, \text{ and } C = \begin{bmatrix} 1 & 0 & 0 & 0 & 0 & 0 & 0 & 0 \\ 0 & 1 & 0 & 0 & 0 & 0 & 0 & 0 \\ 0 & 0 & 1 & 0 & 0 & 0 & 0 & 0 \\ 0 & 0 & 0 & 1 & 0 & 0 & 0 & 0 \\ 0 & 0 & 0 & 0 & 1 & 0 & 0 & 0 \\ 0 & 0 & 0 & 0 & 0 & 1 & 0 & 0 \\ 0 & 0 & 0 & 0 & 0 & 0 & 1 & 0 \\ 0 & 0 & 0 & 0 & 0 & 0 & 0 & 1 \end{bmatrix}
$$

4. Control Design

4.1 The Proportional-Integral-Derivative (PID) Controller

The error between the desired and measured attitude of the above model is defined as follows:

$$
\begin{aligned}
e_1 &= \phi_d - \phi \\
e_2 &= \theta_d - \theta \\
e_3 &= \psi_d - \psi \\
e_4 &= z_d - z
\end{aligned}
\tag{28}
$$

Therefore, the PID controller is applied for each as follows:

$$
v_i = K_{p_i} e_i + K_{I_i} \int_0^t e_i \, d\tau + K_{D_i} \frac{d}{dt} e_i
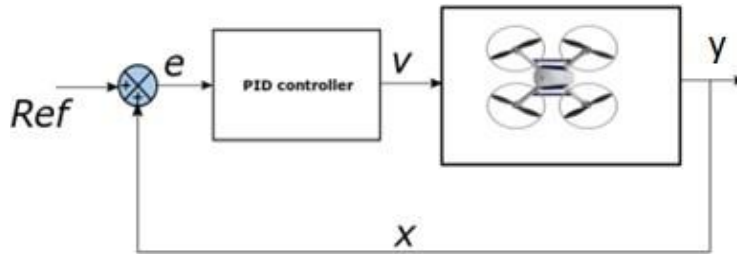\tag{29}
$$

where, i = 1, 2, 3,4

Fig. 5 PID - Controller for the linearized model (closed loop)

4.2 Adaptive Feedback Linearization

Redefining the equations' parameters, (20) can be formulated as follows:

$$
\begin{aligned}
\ddot{\phi} &= a_1 \dot{\theta}\dot{\psi} + a_2 \dot{\theta}\Omega_d + b_1 u_1 \\
\ddot{\theta} &= a_3 \dot{\phi}\dot{\psi} + a_4 \dot{\phi}\Omega_d + b_2 u_2 \\
\ddot{\psi} &= a_5 \dot{\theta}\dot{\psi} + b_3 u_3 \\
\ddot{z} &= -g + \frac{\cos\phi \cos\theta}{m} u_4
\end{aligned}
\tag{30}
$$

By introducing the parameter uncertainties occur in the quadrotor, roll dynamic equation can be rewritten as follow:

$$
\begin{aligned}
\ddot{\phi} &= v_1 + \delta_\phi \\
\ddot{\theta} &= v_2 + \delta_\theta \\
\ddot{\psi} &= v_3 + \delta_\psi \\
\ddot{z} &= v_4 + \delta_z
\end{aligned}
\tag{31}
$$

where, δ_ϕ, δ_θ, δ_ψ and δ_z are the lumped uncertainties which can express as follow [18]:

$$\begin{aligned}
\delta_\phi &= \Delta(a_1)\dot{\theta}\dot{\psi} + \Delta(a_2)\dot{\theta}\Omega_d + \Delta(b_1)u_1 \\
\delta_\theta &= \Delta(a_3)\dot{\phi}\dot{\psi} + \Delta(a_4)\dot{\phi}\Omega_d + \Delta(b_2)u_2 \\
\delta_\psi &= \Delta(a_5)\dot{\theta}\dot{\psi} + \Delta(b_3)u_3 \\
\ddot{z} &= -\Delta(g) + \frac{\cos\phi\cos\theta}{\Delta(m)}u_4
\end{aligned}$$

(32)

Therefore, the errors dynamics are written as follows:

$$\begin{aligned}
e_1 &= \dot{\phi}_d - \dot{\phi} \\
e_2 &= \dot{\theta}_d - \dot{\theta} \\
e_3 &= \dot{\psi}_d - \dot{\psi} \\
e_4 &= \dot{z}_d - \dot{z}
\end{aligned}$$

(33)

And, the error between lumped uncertainties δ_ϕ, δ_θ, δ_ψ and δ_z, and estimated lumped uncertainties $\hat{\delta}_\phi$, $\hat{\delta}_\theta$, $\hat{\delta}_\psi$ and $\hat{\delta}_z$ are written as follows:

$$\begin{aligned}
\tilde{\delta}_\phi &= \hat{\delta}_\phi - \delta_\phi \\
\tilde{\delta}_\theta &= \hat{\delta}_\theta - \delta_\theta \\
\tilde{\delta}_\psi &= \hat{\delta}_\psi - \delta_\psi \\
\tilde{\delta}_z &= \hat{\delta}_z - \delta_z
\end{aligned}$$

(34)

Thus, the following Lyapunov functions are selected to calculate the control laws as follows:

$$\begin{aligned}
V_\phi &= \frac{1}{2}e_\phi^2 + \frac{1}{2}\gamma_\phi\tilde{\delta}_\phi^2 \\
V_\theta &= \frac{1}{2}e_\theta^2 + \frac{1}{2}\gamma_\theta\tilde{\delta}_\theta^2 \\
V_\psi &= \frac{1}{2}e_\psi^2 + \frac{1}{2}\gamma_\psi\tilde{\delta}_\psi^2 \\
V_z &= \frac{1}{2}e_z^2 + \frac{1}{2}\gamma_z\tilde{\delta}_z^2
\end{aligned}$$

(35)

Where γ_ϕ, γ_θ, γ_ψ and γ_z positive constants which called the adaptation law gains. The derivative of (35) is calculated as follows:

$$\begin{aligned}
\dot{V}_\phi &= e_\phi\dot{e}_\phi + \gamma_\phi\dot{\tilde{\delta}}_\phi\tilde{\delta}_\phi \\
\dot{V}_\theta &= e_\theta\dot{e}_\theta + \gamma_\theta\dot{\tilde{\delta}}_\theta\tilde{\delta}_\theta \\
\dot{V}_\psi &= e_\psi\dot{e}_\psi + \gamma_\psi\dot{\tilde{\delta}}_\psi\tilde{\delta}_\psi \\
\dot{V}_z &= e_z\dot{e}_z + \gamma_z\dot{\tilde{\delta}}_z\tilde{\delta}_z
\end{aligned}$$

(36)

If the adaptation laws are selected as follows:

$$\dot{\hat{\delta}}_\phi = -\frac{1}{\gamma_\phi} e_\phi$$
$$\dot{\hat{\delta}}_\theta = -\frac{1}{\gamma_\theta} e_\theta$$
$$\dot{\hat{\delta}}_\psi = -\frac{1}{\gamma_\psi} e_\psi$$
$$\dot{\hat{\delta}}_z = -\frac{1}{\gamma_z} e_z$$

(37)

Then, by substituting (37) into (36) yields to:

$$\dot{V}_\phi = e_\phi \dot{e}$$
$$\dot{V}_\theta = e_\theta \dot{e}_\theta$$
$$\dot{V}_\psi = e_\psi \dot{e}_\psi$$
$$\dot{V}_z = e_z \dot{e}_z$$

(38)

And, by substituting (33) into (38), comes up with the following:

$$\dot{V}_\phi = e_\phi (\ddot{\phi}_d - v_1 - \hat{\delta}_\phi)$$
$$\dot{V}_\theta = e_\theta (\ddot{\theta}_d - v_2 - \hat{\delta}_\theta)$$
$$\dot{V}_\psi = e_\psi (\ddot{\psi}_d - v_3 - \hat{\delta}_\psi)$$
$$\dot{V}_z = e_z (\ddot{z}_d - v_4 - \hat{\delta}_z)$$

(39)

Therefore, the control inputs v_1, v_2, v_3 and v_4 are selected as follow:

$$v_1 = \ddot{\phi}_d - \hat{\delta}_\phi + k_\phi e_\phi$$
$$v_2 = \ddot{\theta}_d - \hat{\delta}_\theta + k_\theta e_\theta$$
$$v_3 = \ddot{\psi}_d - \hat{\delta}_\psi + k_\psi e_\psi$$
$$v_4 = \ddot{z}_d - \hat{\delta}_z + k_z e_z$$

(40)

Leads to:

$$\dot{V}_\phi = -k_\phi e_\phi^2 \le 0$$
$$\dot{V}_\phi = -k_\phi e_\phi^2 \le 0$$
$$\dot{V}_\psi = -k_\psi e_\psi^2 \le 0$$
$$\dot{V}_z = -k_z e_z^2 \le 0$$

(41)

Where k_ϕ, k_θ, k_ψ and k_z are positive constants; therefore (41) shows that the derivative of the selected Lyapunov functions are negative, which prove that the control system is asymptotically stable.

5. Simulation Model

The quadrotor mathematical model has been simulated using Matlab/Simulink platform, and the model parameter values used in this simulation have been selected from [19] and listed in Table 1. The numerical solution of the quadrotor dynamic model and the proposed controllers have been solved using the ode45 variable-step solver (with the default setup). PID and the proposed controller (adaptive feedback linearization) controller's parameters are listed in Table 2 and Table 3, respectively.
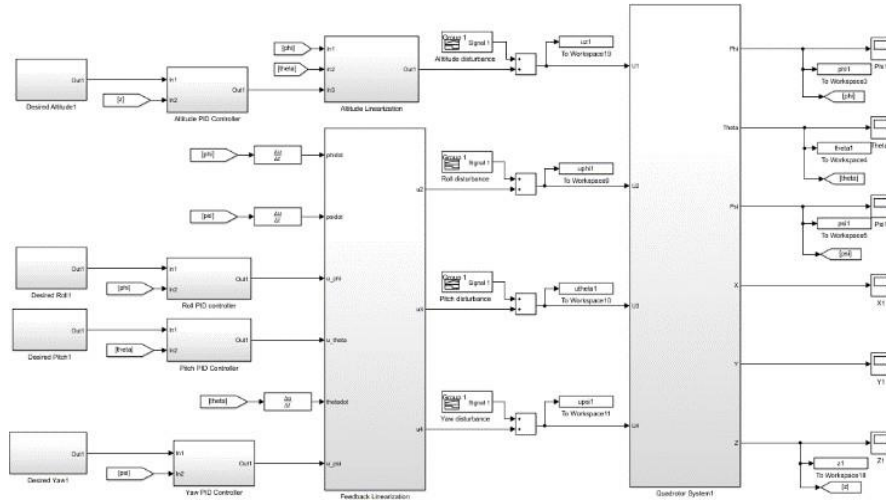
Fig. 6 - The overall Simulink model of the quadrotor UAV and the PID controller
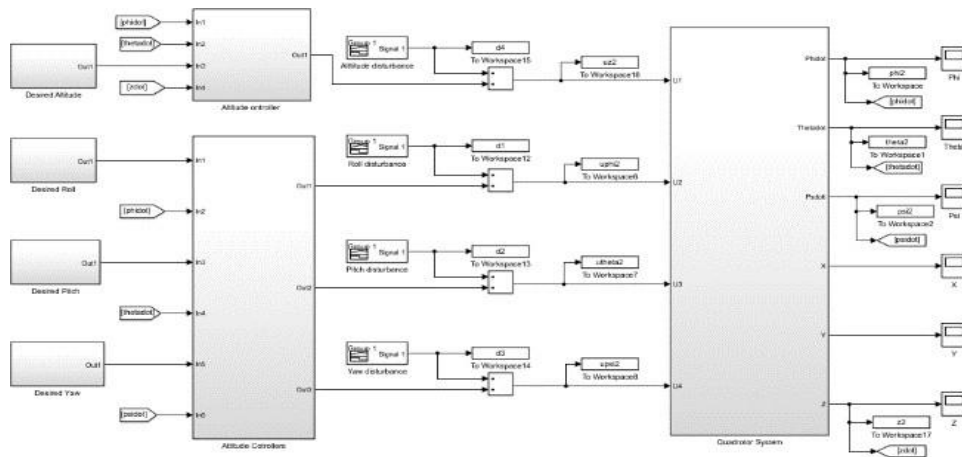

Fig. 7 - The overall Simulink model of the quadrotor UAV and the AFBL controller

Table 1 - Parameters of the quadrotor

Name	Parameter	Value	Unit
mass	m	0.650	kg
inertia on x-axis	I_x	7.5e-3	kgm^2
inertia on y-axis	I_y	7.5e-3	kgm^2
inertia on z-axis	I_z	1.3e-2	kgm^2
thrust coefficient	b	3.13e-5	Ns^2
drag coefficient	d	7.5e-7	Nms^2
rotor inertia	J_r	6e-5	kgm^2
arm length	l	0.23	m

Table 2 - PID Controller Parameters for the Linearized Model

Parameter	z	ϕ	θ	ψ
P	80	30	30	30
I	10	8	8	8
D	10	8	8	8

Table 3 - AFBL Controller Parameters

Parameter	z	ϕ	θ	ψ
γ	20	8	15	8
K	80	8	15	8

1. Simulation Results

The performance of the proposed controller (adaptive feedback linearization) has been evaluated and compared with the conventional exact feedback linearization into two different scenarios in term of trajectory tracking error as follows:

Scenario 1: The ideal case, in which it has been assumed that the obtained mathematical model of the quadrotor is exactly representing the physical quadrotor system. Therefore, the effects of the parameter uncertainty and disturbance have been ignored.

The attitude and altitude of the quadrotor by applying conventional FBL and proposed AFBL has been presented in Fig. 8 and Fig. 9, respectively. While the error in attitude and altitude tracking has been illustrated in Fig. 10 and Fig. 11, respectively, in which the proposed AFBL showed a significant improvement in terms of the trajectory tracking error reduction and results in a robust tracking. For further simulation validation, the reference signals have been changed to sinusoidal (smooth signal), as depicted in Fig. 12, and the associated tracking error is presented in Fig. 13.

Scenario 2: In this case, the performance of the proposed controller has been tested against the presence of the parameter uncertainty occurred in the mass of the quadrotor by applying payload equal up to %50 of the quadrotor mass nominal value; meanwhile, a pulse-type disturbance has been applied into the directions of the attitude and altitude as depicted in Fig. 14 and Fig. 15, respectively.

The attitude and altitude of the quadrotor by applying conventional FBL and the proposed AFBL has been presented in Fig. 16 and Fig. 17, respectively. While the error in attitude and altitude tracking has been illustrated in Fig. 18 and Fig. 19, respectively, in which the proposed AFBL showed a significant improvement in terms of the trajectory tracking error reduction and results in robust tracking even in the presence of the parameter uncertainty and disturbance. For further simulation validation, the reference signals have been changed to sinusoidal (smooth signal), as depicted in Fig. 20, and the associated tracking error is presented in Fig. 21.
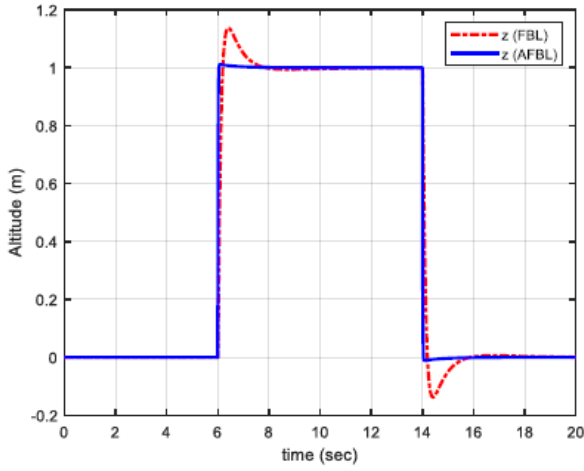
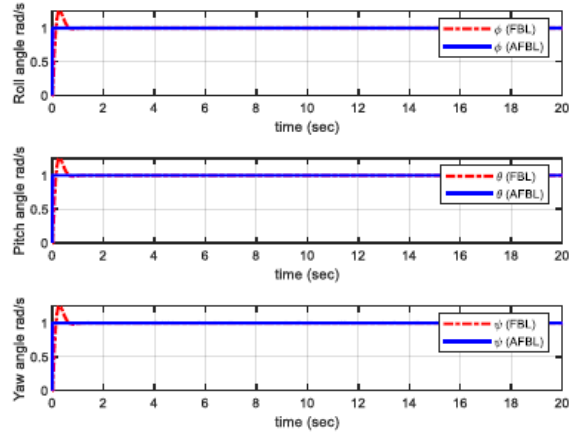**Fig. 8 - Take-off and Landing of the quadrotor UAV using FBL and AFBL Controllers**

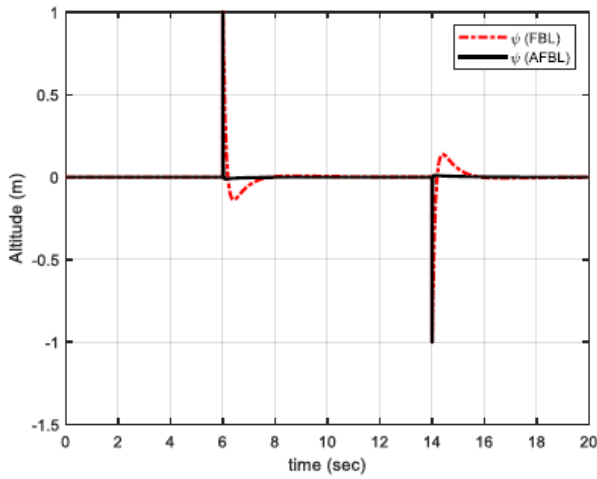**Fig. 9 - Attitude of the quadrotor UAV using FBL and AFBL Controllers**
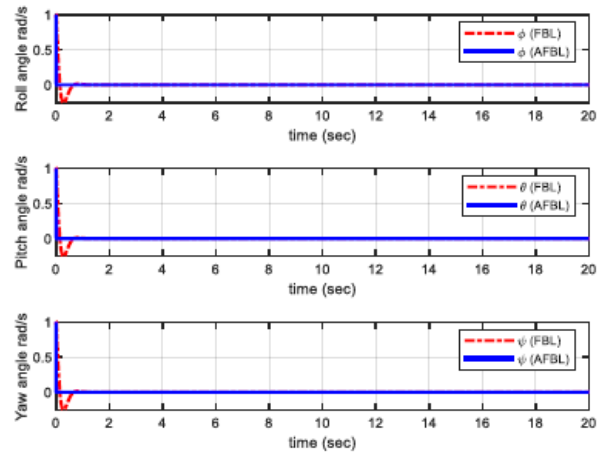

Fig. 10 - Altitude error signal

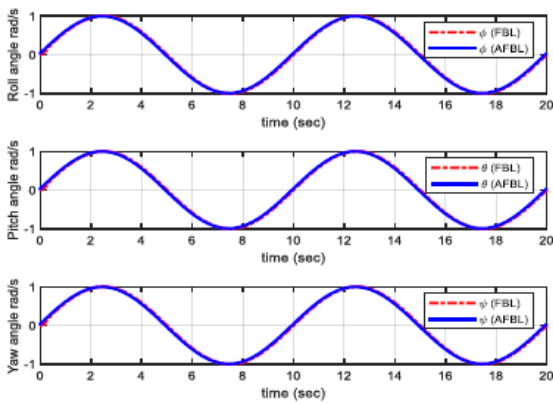**Fig. 11 - Attitude error signals**
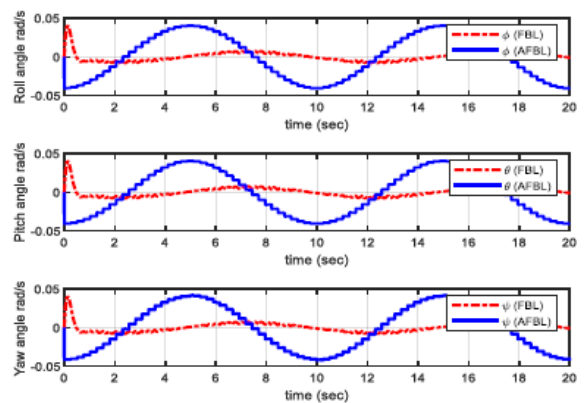

Fig. 12 - Smooth attitude trajectory tracking

Fig. 13 - Attitude error signals under smooth tracking

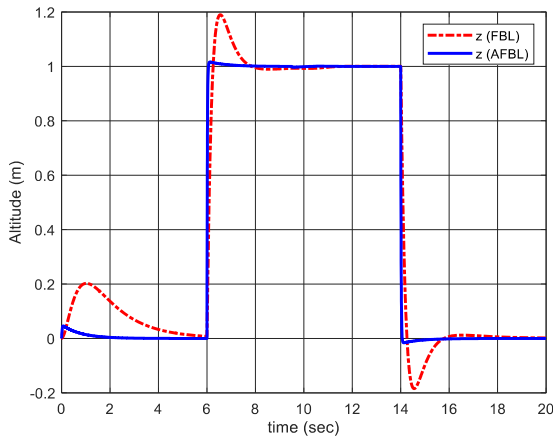**Fig. 14 - Pulse type disturbance on the quadrotor Attitude**

Fig. 15 - Pulse type disturbance on the quadrotor Altitude

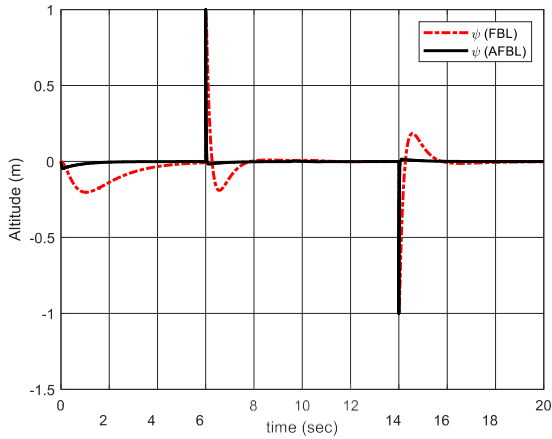**Fig. 16 - Take-off and Landing of the quadrotor UAV using FBL and AFBL Controllers**
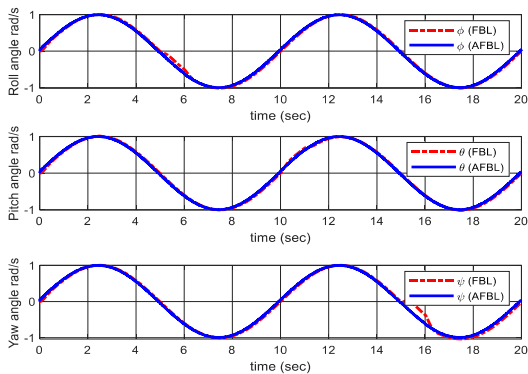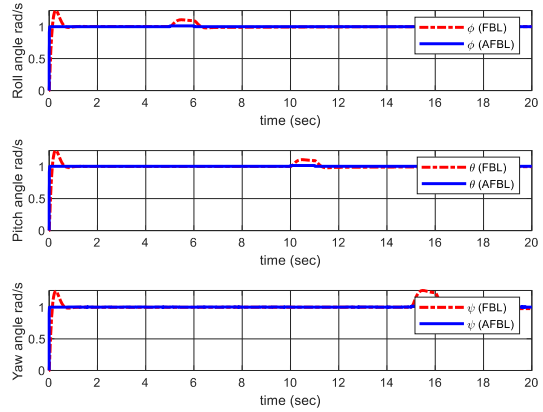
Fig. 17 - Attitude of the quadrotor UAV using FBL and AFBL Controllers

Fig. 18 - Altitude error signal

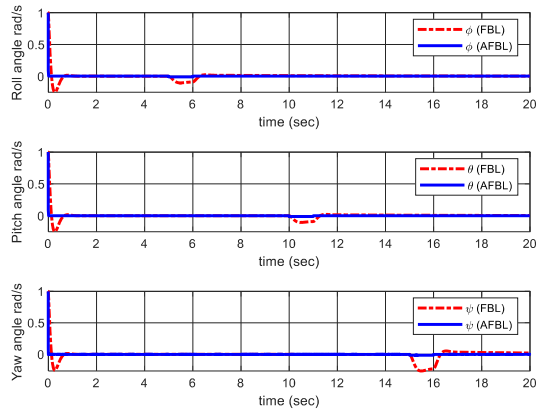**Fig. 19 - Attitude error signals**

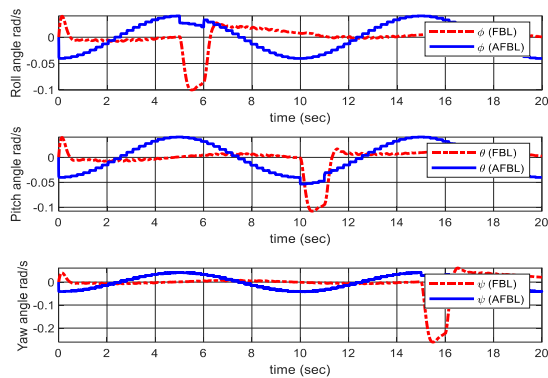**Fig. 20 - Smooth attitude trajectory tracking**

Fig. 21 - Attitude error signals under smooth tracking

For further investigations, the integral square error (ISE) has been calculated based on the (42) for the attitude and (43) for the altitude in both scenarios to measure the performance of the conventional FBL and the proposed AFBL controller values in term of tracking error for scenario 1 and 2, and the results have been presented in Table 1 and Table 2 as follows:

$$ISE(attitude) = \int_0^t (e_\phi^2 + e_\theta^2 + e_\psi^2) dt \tag{42}$$

Table 4 - ISE for the attitude errors

Scenario	*Feedback linearization*	*Adaptive feedback linearization*
ISE value (ideal case)	0.0120	0.0027
ISE value (in case of uncertainty & disturbance)	0.0158	0.0027

As presented in Table 4 and equation (42), the ISE has been calculated for the quadrotor attitude tracking errors for the exact conventional FBL and the proposed AFBL controllers, and the results showed that the proposed AFBL provided a significant improvement by reducing the ISE tracking error from 0.0120 to 0.0027 which is about % 77 reductions (improvement) in the **ideal** case, while in the presence of the parameter uncertainty and disturbance, the ISE tracking error has been reduced from 0.0158 to 0.0027 which is about % 82 improvements.

$$ISE(altitude) = \int_0^t (e_z^2) dt \tag{43}$$

Table 5 - ISE for the altitude errors

Scenario	*Feedback linearization*	*Adaptive feedback linearization*
ISE (ideal case)	0.0155	0.0098
ISE value (in case of uncertainty & disturbance)	0.0214	0.0099

As shown in Table 5 and equation (43), the ISE has been calculated for the quadrotor altitude tracking errors for the exact conventional FBL and the proposed AFBL controllers, and the results showed that the proposed AFBL provided a significant improvement by reducing the ISE tracking error from 0.0155 to 0.0098 which is about % 36 reductions (improvement) in the ideal case, while in the presence of the parameter uncertainty and disturbance, the ISE tracking error has been reduced from 0.0214 to 0.0099 which is about % 53 improvements.

2. Conclusion

The dynamic model of quadrotor UAV has been mathematically presented. The conventional exact feedback linearization technique is used to linearize the attitude and altitude dynamic equations of the quadrotor. The PID controller is applied to the linearized model. However, to improve the performance against the disturbance rejection and the model parameter uncertainties that may occur in the quadrotor system (such as a change in the mass), the adaptive feedback linearization has been proposed and implemented to the attitude and altitude quadrotor system. The stability approach of the proposed controllers has been derived based on the elected Lyapunov function. The simulation results validate that the proposed controller showed a significant improvement in the presence of parameter uncertainty and disturbance.

Acknowledgement

References

[1]   A. Chovancová, T. Fico, E. Chovanec, and P. Hubinský, "Mathematical modelling and parameter identification of quadrotor (a survey)," *Procedia Eng.*, vol. 96, no. October, pp. 172–181, 2014.

[2]   A. Rodić and G. Mester, "Modeling and simulation of quad-rotor dynamics and spatial navigation," SISY 2011 - 9th Int. Symp. Intell. Syst. Informatics, Proc., pp. 23–28, 2011.

[3]   Y. Naidoo, R. Stopforth, and G. Bright, "Quad-Rotor Unmanned Aerial Vehicle Helicopter Modelling & Control," *Int. J. Adv. Robot. Syst.*, vol. 8, no. 4, pp. 139–149, 2011.

[4]   K. U. Lee, Y. H. Yun, W. Chang, J. B. Park, and Y. H. Choi, "Modeling and Altitude Control of Quad-rotor UAV," *Int. Conf. Control. Autom. Syst. Oct. 26-29, 2011 KINTEX*, pp. 1897–1902, 2011.

[5]   H. Lee and H. J. Kim, "Trajectory tracking control of multirotors from modelling to experiments: A survey," *Int. J. Control. Autom. Syst.*, vol. 15, no. 1, pp. 281–292, 2017.

[6]   A. L. Salih, M. Moghavvemi, H. A. F. Mohamed, and K. S. Gaeid, "Modelling and PID controller design for a quadrotor unmanned air vehicle," *2010 IEEE Int. Conf. Autom. Qual. Testing, Robot. AQTR 2010 - Proc.*, vol. 1, pp. 74–78, 2010.

[7]   B. C. Min, C. H. Cho, K. M. Choi, and D. H. Kim, "Development of a micro quad-rotor UAV for monitoring an indoor environment," *Lect. Notes Comput. Sci. (including Subser. Lect. Notes Artif. Intell. Lect. Notes Bioinformatics)*, vol. 5744 LNCS, pp. 262–271, 2009.

[8]   J. Li and Y. Li, "Dynamic analysis and PID control for a quadrotor," *2011 IEEE Int. Conf. Mechatronics Autom. ICMA 2011*, pp. 573–578, 2011.

[9]   A. L. Salih, M. Moghavvemi, H. A. F. Mohamed, and K. S. Gaeid, "Flight PID controller design for a UAV quadrotor," *Sci. Res. Essays*, vol. 5, no. 23, pp. 3660–3667, 2010.

[10]   A. Ataka, H. Tnunay, R. Inovan, M. Q. Abdurrohman, H. Prestianto, A. Cahyadi, and Y. Yamamoto, "Controllability and observability analysis of the gain scheduling based linearization for UAV quadrotor," *Proc. 2013 Int. Conf. Robot. Biomimetics, Intell. Comput. Syst. ROBIONETICS 2013*, no. November, pp. 212–218, 2013.

[11]   T. Madani and A. Benallegue, "Backstepping control for a quadrotor helicopter," *IEEE Int. Conf. Intell. Robot. Syst.*, no. May 2016, pp. 3255–3260, 2006.

[12]   P. Mukherjee and S. Waslander, "Direct Adaptive Feedback Linearization for Quadrotor Control," *AIAA Guid. Navig. Control Conf. 2012*, no. August, pp. 1–10, 2012.

[13]   D. Lee, H. J. Kim, and S. Sastry, "Feedback linearization vs. adaptive sliding mode control for a quadrotor helicopter," *Int. J. Control. Autom. Syst.*, vol. 7, no. 3, pp. 419–428, 2009.

[14]   H. Voos, "Nonlinear control of a quadrotor micro-uav using feedback-linearization," *IEEE 2009 Int. Conf. Mechatronics, ICM 2009*, no. April, pp. 4–9, 2009.

[15]   M. Mardan, M. Esfandiari, and N. Sepehri, "Attitude and position controller design and implementation for a quadrotor," *Int. J. Adv. Robot. Syst.*, vol. 14, no. 3, pp. 1–11, 2017.

[16]   Carlos, Bárbara B., Antonio É. RM de Oliveira, R. Auzuir, Rejane C. Sá, and Antonio WO Rodrigues, "Modeling, Control and Simulation of a Quadrotor for Attitude Stabilization," *In Workshop on Engineering Applications,* Sep 27, pp. 12-23. Springer, Cham, 2017.

[17]   R. Olfati-Saber, "Nonlinear Control of Underactuated Mechanical Systems with Application to Robotics and

Aerospace Vehicles," *Thesis PhD*, p. 307, 2001.

[18]   J. Soltani and M. M. Rezaei, "Robust control of an islanded multi-bus microgrid based on input–output feedback linearisation and sliding mode control," *IET Gener. Transm. Distrib.*, vol. 9, no. 15, pp. 2447–2454, 2015.

[19]   S. Bouabdallah, "Design and control of quadrotors with application to autonomous flying," *Ph.D. Thesis*, Ecole Polytechnique Federale de Lausanne, 2007.